International Journal of Nanomedicine

Dovepress
open access to scientific and medical research

Open Access Full Text Article

ORIGINAL RESEARCH

Nanostructured delivery system for zinc phthalocyanine: preparation, characterization, and phototoxicity study against human lung adenocarcinoma A549 cells

This article was published in the following Dove Press journal:
International Journal of Nanomedicine
24 January 2011
Number of times this article has been viewed

Mariana da Volta Soares[1]
Mainara Rangel Oliveira[1]
Elisabete Pereira dos Santos[1]
Lycia de Brito Gitirana[2]
Gleyce Moreno Barbosa[3]
Carla Holandino Quaresma[3]
Eduardo Ricci-Júnior[1]

[1]Department of Medicines, Laboratório de Desenvolvimento Galênico (LADEG), Faculty of Pharmacy, [2]Laboratory of Animal and Comparative Histology, Glycobiology Research Program, Institute of Biomedical Science, [3]Department of Medicines, Laboratório Multidisciplinar de Ciências Farmacêuticas, Faculty of Pharmacy, Federal University of Rio de Janeiro (UFRJ), Rio de Janeiro, Brazil

Abstract: In this study, zinc phthalocyanine (ZnPc) was loaded onto poly-ε-caprolactone (PCL) nanoparticles (NPs) using a solvent emulsification–evaporation method. The process yield and encapsulation efficiency were 74.2% ± 1.2% and 67.1% ± 0.9%, respectively. The NPs had a mean diameter of 187.4 ± 2.1 nm, narrow distribution size with a polydispersity index of 0.096 ± 0.004, zeta potential of –4.85 ± 0.21 mV, and spherical shape. ZnPc has sustained release, following Higuchi's kinetics. The photobiological activity of the ZnPc-loaded NPs was evaluated on human lung adenocarcinoma A549 cells. Cells were incubated with free ZnPc or ZnPc-loaded NPs for 4 h and then washed with phosphate-buffered saline. Culture medium was added to the wells containing the cells. Finally, the cells were exposed to red light (660 nm) with a light dose of 100 J/cm^2. The cellular viability was determined after 24 h of incubation. ZnPc-loaded NPs and free photosensitizer eliminated about 95.9% ± 1.8% and 28.7% ± 2.2% of A549 cells, respectively. The phototoxicity was time dependent up to 4 h and concentration dependent at 0–5 μg ZnPc. The cells viability decreased with the increase of the light dose in the range of 10–100 J/cm^2. Intense lysis was observed in the cells incubated with the ZnPc-loaded NPs and irradiated with red light. ZnPc-loaded PCL NPs are the release systems that promise photodynamic therapy use.

Keywords: photosensitizer, nanoparticles, photodynamic therapy, lung cancer, phototoxicity, biodistribution

Introduction

Photodynamic therapy (PDT) is being actively exploited in many clinical applications such as cancer treatment, age-related macular degeneration, and infection.[1,2] PDT is based on the administration of drugs known as photosensitizers that are taken up and/or retained by neoplastic tissues.[3,4] The photosensitizers alone are harmless and ideally have no effect on either healthy or abnormal tissues. After a predefined time interval that allows photosensitizer accumulation in the tumor tissue, the illumination of the tumor site with nonthermal light (600–800 nm) leads to the formation of an excited photosensitizer. The combined action of the excited triplet photosensitizer and molecular oxygen results in the formation of singlet oxygen ($^1O_2$), which is the main mediator of cellular death induced by PDT.[2] PDT has been shown to induce both apoptosis (slow process)[5] and necrosis (drastic process).[3] Among the most promising second-generation photosensitizers for PDT are the phthalocyanines. In this study, zinc phthalocyanine (ZnPc), a metallophthalocyanine, was used because of its very

Correspondence: Eduardo Ricci-Júnior
Department of Medicines, Laboratório de Desenvolvimento Galênico (LADEG), Faculty of Pharmacy, Federal University of Rio de Janeiro (UFRJ), Carlos Chagas Filho Avenue, Rio de Janeiro, RJ 21941-590, Brazil
Tel +55 21 2262 6625
Fax +55 21 2260 7381
Email ricci@pharma.ufrj.br

submit your manuscript | www.dovepress.com
Dovepress
DOI: 10.2147/IJN.S15860

strong phototoxicity effect,[6] easy availability, and low cost. ZnPc is stable and produces $^1O_2$ with high yield.[7] However, ZnPc is lipophilic and slightly soluble in water or in a physiologically acceptable vehicle. This hydrophobic characteristic hinders its systemic administration and restricts its clinical studies.

ZnPc is a dye and photosensitizer with molecular weight of 577.91 g/mol. It is a crystalline powder, lipophilic, and soluble in pyridine, dimethylsulfoxide, dimethylformamide, and dichloromethane (DCM).[8] The photosensitizer can be dissolved in dimethylsulfoxide and diluted with ethanol. However, it suffers aggregation in water with reduction of its photobiological activity.[9] It exhibits a high thermal stability, and <5% of its mass is lost at 500°C.[9] ZnPc has strong absorbance in the red region of the spectrum of visible light (λ_{max} = 666 nm in ethanol). It has strong fluorescence emission in the range of 650–800 nm.[9] Methylene blue (MB) is a hydrophilic dye and photosensitizer.[10] In this study, it was used as a positive control of the photobiological activity. It exhibits strong absorbance in the red region (λ_{max} = 656 nm in water) and fluorescence emission (λ_{max} = 656 nm)[10] similar to ZnPc.

Nanoparticles (NPs) are promising delivery systems for use in PDT. These systems provide sustained release, avoid plasmatic fluctuations, decrease side effects, reduce the frequency of administration, and enhance the uptake of drugs by targeted tissue, increasing the treatment effectiveness.[2,11–14] Advances in nanobiotechnology have resulted in the development of several colloidal carrier systems such as NPs to achieve these multiple objectives.[2,4] The encapsulation of hydrophobic drugs in NPs is a viable alternative in solving the solubility problem,[12] besides promoting targeted delivery and sustained release. The liposomes and the nanoemulsions are examples of drugs carrier. However, they have problems of physical stability. The liposomes can suffer disruption and have limited capacity to encapsulate lipophilic drugs.[15] Nanoemulsions can suffer creaming, flocculation, and coalescence. NPs have excellent physical stability, provide protection of the actives, and sustain drugs release.[15]

NPs have been used as a vehicle for the delivery of PDT agents.[2,4,16,17] Several photosensitizers, many of which are hydrophobic, have been encapsulated in polyesters, such as poly(lactic-co-glycolic acid) and polylactic acid NPs, to overcome the problems associated with solubilization.[12] For example, meso-tetra(4-hydroxyphenyl) porphyrin,[18,19] bacteriochlorophyll-a,[20] verteporfin,[21] MB,[22] hypericin,[23] and various phthalocyanines[9,24] have all been encapsulated in such polyesters. Several studies have proved that the NPs are promising delivery systems for photosensitizers. Generally, photosensitizers loaded in NPs induce better phototoxicity than free photosensitizers.[18,23] Moreover, encapsulation in NPs decreases the aggregation of the photosensitizer in solution[20] or in physiologically acceptable vehicles.

Biocompatible and biodegradable polymers can be used to produce NPs. Much attention has been focused on poly-ε-caprolactone (PCL), a semicrystalline polyester.[9,25–27] This polymer has been used in the development of release systems such as microparticles and NPs.[25–27] PCL NPs have been used as delivery systems of isradipine,[28] primidone,[29] paclitaxel,[30] griseofulvin,[31] tamoxifen,[32] espironolactone,[33] vinblastine,[34] and docetaxel.[35]

The aim of this study was to load ZnPc in PCL NPs to improve the photobiological activity of the photosensitizer. NPs were produced and characterized in terms of their size, charge, morphology, and encapsulation efficiency (EE). In vitro release studies were carried out to evaluate the photosensitizer release profile and kinetic study. The photobiological activity of the ZnPc-loaded NPs and free photosensitizer were assessed on human lung adenocarcinoma A549 cancer cells.

Material and methods

Materials

ZnPc (M_W = 577.91), MB (M_W = 373.90) (≥82%), hydrolyzed polyvinyl alcohol (PVA) (87%–89%) (M_W = 13,000–23,000), 9,10-anthracenediyl-bis(methylene)dimalonic acid (ABMDMA), 3-(4,5-dimethyl-thiazol-2-yl)-2,5-biphenyl tetrazolium bromide (MTT), and PCL (M_W = 42,500–65,000) were purchased from Sigma-Aldrich (St. Louis, MO). DCM and acetone were purchased from Merck (Darmstadt, Germany). Sodium dodecyl sulfate (SDS), NaCl, KCl, NaH_2PO_4, and Na_2HPO_4 were purchased from Vetec (Duque de Caxias, Brazil). Uranyl acetate was purchased from Reagem (Colombo, Brazil). The following cell culture items were purchased from Gibco Invitrogen (New York, NY): Dulbecco's modified Eagle's medium (DMEM), glutamine, fetal bovine serum (FBS), sodium bicarbonate, sodium hydroxide, and Pen Strep (penicillin 10,000 units/mL + streptomycin 10,000 μg/mL in aqueous solution).

NPs preparation and process yield (%)

NPs were prepared by the emulsification and solvent evaporation method. Briefly, ZnPc (3 mg) and PCL (97 mg) were dissolved in the DCM (8 mL). The organic solution was

emulsified in 50 mL of aqueous solution of PVA (1.5%, w/w), for 5 min using an ultrasonicator UP100H (100 W, 30 kHz) (Hielscher, Teltow, Germany) in an ice bath. PVA is a biocompatible polymer and has the function of a surfactant. DCM was evaporated under reduced pressure using a rota vapor (Heidolph, Schwabach, Germany) at room temperature (28°C). The NPs were purified thrice by centrifugation at 20,000 *g* (Avanti J-25; Beckman Coulter, San Francisco, CA) for 20 min followed by resuspension in water to remove the surfactant. NPs were then transferred into glass vials, frozen in a liquid nitrogen bath, and lyophilized (Lyophilizer, FreeZone 4.5-L Benchtop Freeze Dry System; Labconco, Kansas City, MO). The lyophilized powder was stored at room temperature (28°C) before analysis.

The process yield (%, w/w) was calculated by Eq. 1:

$$Y(\%) = \frac{M_1}{M_2} \times 100, \quad (1)$$

where Y(%) is the process yield, M_1 is the mass of recovered lyophilized powder, and M_2 is the mass of the formulation (PCL and ZnPc).

Characterization

NPs were characterized in terms of their size, polydispersity index (PI), morphology, surface charge, EE, and drug content (DC). The size and PI were determined by photon correlation spectroscopy using a Zetasizer® 5000 (Malvern Instruments, Malvern, UK). Before measurements, the lyophilized powders were diluted using purified water. The surface charge (zeta potential) was measured using the electrophoretic mode with the Zetasizer 5000. The lyophilized powder was dispersed in water. The pH of the suspension was measured at room temperature (28°C). Morphology was evaluated by transmission electron microscopy (TEM) (Morgagni 268; FEI, Hillsboro, OR). Lyophilized powder was dispersed in water and 5 µL was transferred to a grid. Uranyl acetate solution (3%) was added for fixing and contrast. After 30 sec, excess liquid was removed using filter paper (Whatman®; Maidstone, Kent, UK). Grids were placed in vacuum desiccators (Pyrex®; Corning, Lowell, MA) before analysis.

The drug extraction method from NPs was patronized for determination of the EE and DC. The lyophilized powder was added in hot acetone (45°C) for disruption of the NPs and dissolution of the photosensitizer. The organic solution was sonicated for 10 min using an ultrasonic bath (T14; Thornton, Vinhedo, São Paulo, Brazil). The organic solution was diluted in phosphate-buffered saline (PBS) containing 2% SDS to precipitate the polymer (PCL) and to extract the photosensitizer. The suspension was centrifuged, filtered through a membrane filter (0.45 µm, Millex-FH_{50} filter unit; Millipore, Billerica, MA) to remove the PCL, and quantified by fluorescence emission. The photosensitizer was diluted in PBS containing 2% SDS at concentrations of 20–200 ng/mL. The solutions were excited at 610 nm, and fluorescence emission was measured at 680 nm using a Jasco FP-750 fluorimeter (Jasco Corporation, Tokyo, Japan). The determination coefficient (R^2) exceeded 0.999, with excellent linearity. Intraday and interday precision and accuracy of the method showed a variation coefficient and a relative error (E) not >2.3% and 3.1%, respectively.

EE was calculated from Eq. 2:

$$\mathrm{EE}(\%) = \frac{M_3}{M_4} \times 100, \quad (2)$$

where EE(%) is the encapsulation efficiency, M_3 is the mass of ZnPc measured in lyophilized powder, and M_4 is the mass of photosensitizer used in formulation.

DC in the NPs (µg ZnPc/mg NP) was calculated from Eq. 3:

$$\mathrm{DC}\left(\frac{\mu g\ \mathrm{ZnPc}}{\mathrm{mg\ Np}}\right) = \left(\frac{M_5}{M_6}\right), \quad (3)$$

where DC is the drug content, M_5 is the mass (µg) of ZnPc measured in lyophilized powder, and M_6 is the mass (mg) of the lyophilized NP.

In vitro releasing studies and kinetic

A known amount of NPs (50 mg NP containing 1 mg of ZnPc) was dispersed in 60 mL of PBS containing 0.5% SDS, with pH 7.4, kept at 37°C in a thermostatic bath (M214M2; Quimis, Diadema, São Paulo, Brazil). The acceptor solution was stirred with a magnetic stirrer at a constant rate of 300 rpm using a stirrer (M15; Marte, Santa Rita do Sapucaí, Minas Gerais, Brazil). At given time intervals, six samples (n = 6) of 3 mL were withdrawn and centrifuged at 20,000 *g* for 20 min. The precipitates were resuspended in 3 mL of fresh medium and placed in the respective dissolution vessels. The released photosensitizer was quantified by fluorescence emission. The in vitro release profile was obtained by correlating time (h) versus drug release (%).

After 240 h of release studies, the acceptor solution containing the NPs was removed from the dissolution vessel and centrifuged thrice at 20,000 *g* for 20 min to recover the nanostructured system. The NPs were lyophilized, and the photosensitizer content was determined by fluorescence emission. The extraction and quantification of the photosensitizer of the lyophilized NPs have been described in the 'Characterization' section.

The release data were fitted using the mathematical models of zero order, first order, Higuchi, Hixon–Crowell, square root of mass, three seconds root of mass, and Baker–Lonsdale.[36,37] Equations of the mathematical modeling are shown in Table 1. The data were fitted, and the linear regression was assessed. The correlation coefficient (r) and R^2 were compared to determine the mathematical model that best fits the release data.

In vitro photobiological activity

The human lung adenocarcinoma cell line (A549)[38] was chosen for evaluation of the photobiological activity. The cells were thawed and placed in DMEM supplemented with 10% FBS. Penicillin (100 units/mL) and streptomycin (100 μg/mL) were added to the culture medium. The medium was maintained at 37°C in a 5% CO_2 atmosphere for 48 h. Cell concentrations were determined by the exclusion test of trypan blue using a Neubauer counting chamber. Aliquots of 1×10^5 cells/mL were placed into 96-well dishes containing 250 μL of culture medium. The cell culture was incubated for 24 h at 37°C in a 5% CO_2 atmosphere before examination of the toxicity and phototoxicity of the free photosensitizer, and the photosensitizer was loaded in NPs.

An NP suspension was prepared in culture medium (DMEM) at 1 mg/mL. The cells were washed with PBS and incubated with 250 μL of the NP suspension (dose = 5 μg of ZnPc) at 37°C in a 5% CO_2 atmosphere for 4 h. After incubation, the cells were washed twice with PBS and fresh culture medium (250 μL) was added in each well. Finally, after cellular uptake of the free ZnPc or ZnPc-loaded NPs, the cells were exposed to red light (660 nm) for 90 sec, with a light dose of 100 J/cm^2 (Photon Lase I; DMC, São Carlos, São Paulo, Brazil). After light exposure, the cell culture was incubated for 24 h at 37°C in a 5% CO_2 atmosphere, and the cellular viability was determined by MTT assay. The NP suspension without photosensitizer (empty NPs), control (PBS) solution, and photosensitizer solution were also assessed in the phototoxicity studies. The dark toxicity was also assessed with the same samples. The photobiological activity of the light was evaluated. The cell culture was exposed to red light (660 nm) with light dose of 0–100 J/cm^2, and cell viability was determined by the MTT assay. Briefly, after removing the cell medium, 50 μL of MTT solution (1 mg/mL) was added to each well and incubated for 3 h.[39] Then, the formazan crystals were dissolved with 100 μL of 10% SDS in 0.01 M HCl in each well.[39] The absorbance was determined at 595 nm by a microplate reader. For each sample, the cellular viability was calculated from the data of 10 wells (n = 10) and expressed as a percentage, compared with the untreated cells (100%). Comparison of the mean optical density between the untreated (100%) and treated cells 24 h after illumination allowed the evaluation of the phototoxicity.

MB was used as a positive control of the photobiological activity. The influence of different parameters on the in vitro phototoxicity was investigated by varying the time (1–6 h), concentration of photosensitizer (0–10 μg), and light dose (0–100 J/cm^2).

Table 1 Mathematical models used for linearization of the photosensitizer release profile data

Mathematical models	Equation
Zero order	$F = k_0 t$
First order	$\ln(1 - F) = -k_f t$
Higuchi	$F = k_H t^{1/2}$
Baker–Lonsdale	$3/2[1 - (1 - F)^{2/3}] - F = k_{3/2} t$
Hixon–Crowell	$1 - (1 - F)^{1/3} = k_{1/3} t$
Square root of mass	$1 - (1 - F)^{1/2} = k_{1/2} t$
Three seconds root of mass	$1 - (1 - F)^{2/3} = k_{2/3} t$

Notes: F denotes fraction (%) of drug released up to time t. k_0, k_f, k_H, $k_{3/2}$, $k_{1/3}$, $k_{1/2}$, and $k_{2/3}$ are constants of the mathematical models.

Morphological evaluation

Aliquots of 1×10^5 cells/mL were placed in 24-well dishes containing culture medium. A coverslip was placed on the bottom of the well for growth of cells in monolayer. The cell culture was incubated for 24 h at 37°C in a 5% CO_2 atmosphere before phototoxicity assay. The cells were washed with PBS and incubated with NPs suspension (dose = 5 μg of ZnPc) (at 37°C in a 5% CO_2 atmosphere) for 4 h. After incubation, the cells were washed twice with PBS. Culture medium was added in each culture plate. Finally, the cells were exposed to red light (660 nm) for 90 sec (light dose of 100 J/cm^2) and incubated for 24 h (at 37°C in a 5% CO_2 atmosphere) before microscopic analysis. The empty NPs and control solution (PBS) were also assessed.

For microscopic analysis, the cells were fixed in Bouin's liquid for 5 min and washed with alcohol (70%, v/v) and water

to remove the fixative solution. The cells were stained with Giemsa's liquid for 2 h.[40] Then, the cells were treated and dehydrated with glacial acetic acid, acetone, acetone–xylene (7:3, v/v), acetone–xylene (1:1, v/v), acetone–xylene (3:7, v/v), and xylene. The coverslips were dried and mounted on glass slides for observation under light microscope (DML30; Leica, Bannockburn, IL). The morphology was evaluated for detection of changes in the cytoplasm and nucleus.

$^1O_2$ detection by photobleaching

The $^1O_2$ generation was determined by photobleaching of the chemical probe ABMDMA. It is a water-soluble derivative of anthracene that can react with $^1O_2$ to yield an endoperoxide, which causes a decrease in the ABMDMA absorption.[41] The reaction was monitored spectrophotometrically by recording the decrease in absorption at 400 nm (wavelength of maximum absorption). In this study, 0.15 mM of the sodium salt of ABMDMA in water was mixed with 5 μg of the encapsulated ZnPc or free ZnPc. The empty NPs were used as control. The solution was irradiated with red light (660 nm) (Photon Lase I; DMC) in an open quartz cell with continuous stirring. The absorbance measurements followed by irradiation were carried out every 60 sec.

Statistical analysis

The encapsulation method, process yield, size, PI, surface charge, EE, DC, and $^1O_2$ detection by photobleaching were accomplished in triplicate (n = 3). The in vitro release studies and kinetics were carried out to six determinations (n = 6). The cellular viability was calculated from the data of 10 wells (n = 10) and expressed as a percentage, compared with the untreated cells (100%). All results were expressed as the means ± standard deviation. The statistical comparisons of the photobiological activity were performed using Student's *t*-test. The differences were considered significant at a level of $P < 0.05$.

Results

The process yields of the empty NPs and ZnPc-loaded NPs were 73.5% ± 1.8% and 74.2% ± 1.2% (w/w), respectively. The EE of ZnPc in PCL NPs was about 67.1% ± 0.9%. Besides, the ZnPc content of NPs was 20.1 ± 0.07 μg/mg. The ZnPc-loaded NPs had an average size of 187.4 ± 2.1 nm. Compared with empty NPs (179 ± 1.5 nm), photosensitizer-loaded NPs had a larger size. IP of the empty NPs and ZnPc-loaded NPs was of 0.102 ± 0.02 and 0.096 ± 0.004, respectively. The empty NPs and ZnPc-loaded NPs exhibited negative zeta potential of −3.4 ± 0.08 and −4.85 ± 0.21 mV, respectively. The morphology of the particles was examined by TEM and is shown in Figure 1. The ZnPc-loaded NPs were spherical (Figure 1A). Figure 1C shows the PCL NPs, which were isolated and magnified. Figures 1B and 1D are photomicrographs of empty NPs.

The in vitro release studies are shown in Figure 2A. ZnPc has a sustained release. Besides, 22% of the photosensitizer was released from the NPs in 240 h.

After in vitro release studies, the remaining content (%) of ZnPc in the PCL NPs was assessed to compare with released photosensitizer in the acceptor solution. Table 2 shows the data of the total of the released ZnPc and the remaining content (%, w/w) of ZnPc in the PCL NPs. The remaining content of the drug in the NPs confirms and validates the release data, showing that in vitro release studies were suitable for the delivery system.

Several mathematical models were used to investigate the mechanism of drug release from PCL NPs. Thus, linear regression of the release data was performed using the mathematical models of zero order, first order, Higuchi, Hixon–Crowell, square root of mass, three seconds root of mass, and Baker–Lonsdale. The R^2 and r values obtained after linear regression are shown in Table 3.

Kinetic models were established to describe the release kinetics and understand the mechanism of drug release from delivery systems.[36,37] As shown in Table 3 and Figure 2B, the Higuchi model gave the highest value of R^2 and r, indicating that this mathematical model was the most suitable for

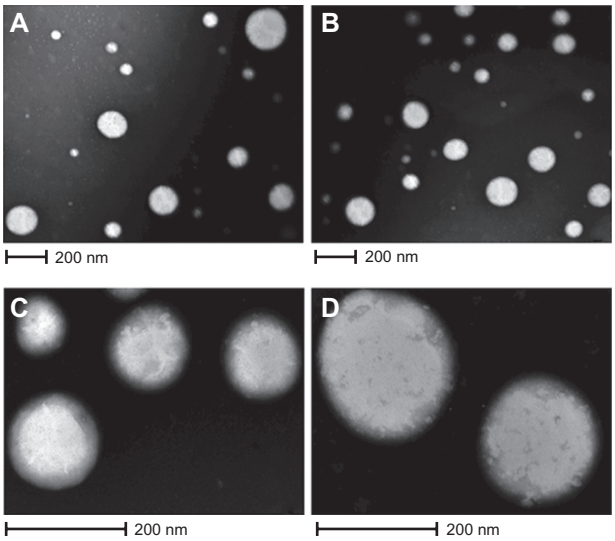

Figure 1 Photographs of TEM. **A**) and **C**) ZnPc-loaded PCL nanoparticles; **B**) and **D**) empty nanoparticles.
Abbreviations: TEM, transmission electron microscopy; ZnPc, zinc phthalocyanine; PCL, poly-ε-caprolactone.

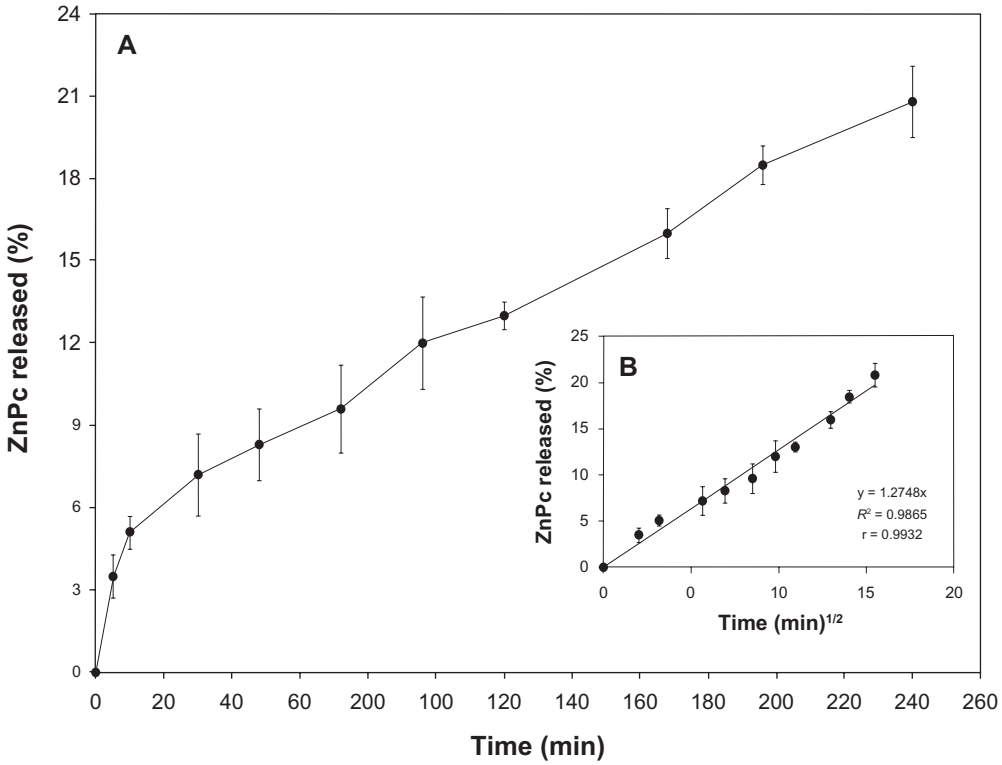

Figure 2 A) In vitro releasing profile of the ZnPc from nanostructured system. **B**) Graphic representation of the Higuchi model obtained after regression. Mean and SD of n = 6 determinations.
Abbreviations: ZnPc, zinc phthalocyanine; SD, standard deviation.

describing the release of the photosensitizer from PCL NPs. These results suggest that the release of ZnPc from PCL NPs is controlled by diffusion.

The photobiological activity at different incubation times of free ZnPc, free MB, and ZnPc-loaded NPs is shown in Figure 3. No toxicity was observed in the dark. The phototoxicity was time dependent up to 4 h. No significant difference ($P > 0.05$) in the phototoxicity of the encapsulated ZnPc was observed for the incubation time of 4 and 6 h. Thus, the incubation time of 4 h was chosen for other phototoxicity studies (influence of the light dose and concentration). The cell viability of the free ZnPc slowly decreased in the range 1–6 h. The photobiological activity of the MB was observed after 2 h of incubation with activity maximum in 6 h. ZnPc-loaded NPs exhibited phototoxicity significantly higher than free photosensitizers ($P < 0.05$) (Figure 3).

Table 2 Released drug in the acceptor solution and remaining content of photosensitizer in the nanoparticles

Released drug (%)[1]	Remaining drug in the nanoparticles (%)[1]	Total (%)[2]	Loss (%)[2]
22.1 ± 0.24	70.8 ± 0.48	92.9	7.1

Notes: [1]Media ± standard deviation of n = 6 determinations; [2]Media of n = 6 determinations.

The photobiological activity of different concentrations of ZnPc-loaded NPs was evaluated in cell cultures and compared with the free photosensitizers. MB was used as control. No toxicity was observed in the dark. In the assays without photosensitizer, ZnPc-loaded NPs and free photosensitizer were replaced by empty NPs and PBS, respectively. The cell viability decreased with the increase in drug concentration (Figure 4). No significant difference ($P > 0.05$) in the photobiological activity of the encapsulated ZnPc was observed for the concentrations of 5 and 10 μg/mL. The phototoxicity of the free ZnPc was not concentration dependent (Figure 4). The phototoxicity of the MB was observed only

Table 3 Determination coefficient (R^2) and correlation coefficient (r) obtained after linear regression of the release data

Mathematical models	R^2	r
Zero order	0.9556	0.9775
First order	0.9663	0.9830
Higuchi	0.9861	0.9932
Baker–Lonsdale	0.9782	0.9890
Hixon–Crowell	0.9629	0.9812
Square root of mass	0.9612	0.9824
Three seconds root of mass	0.9594	0.9794

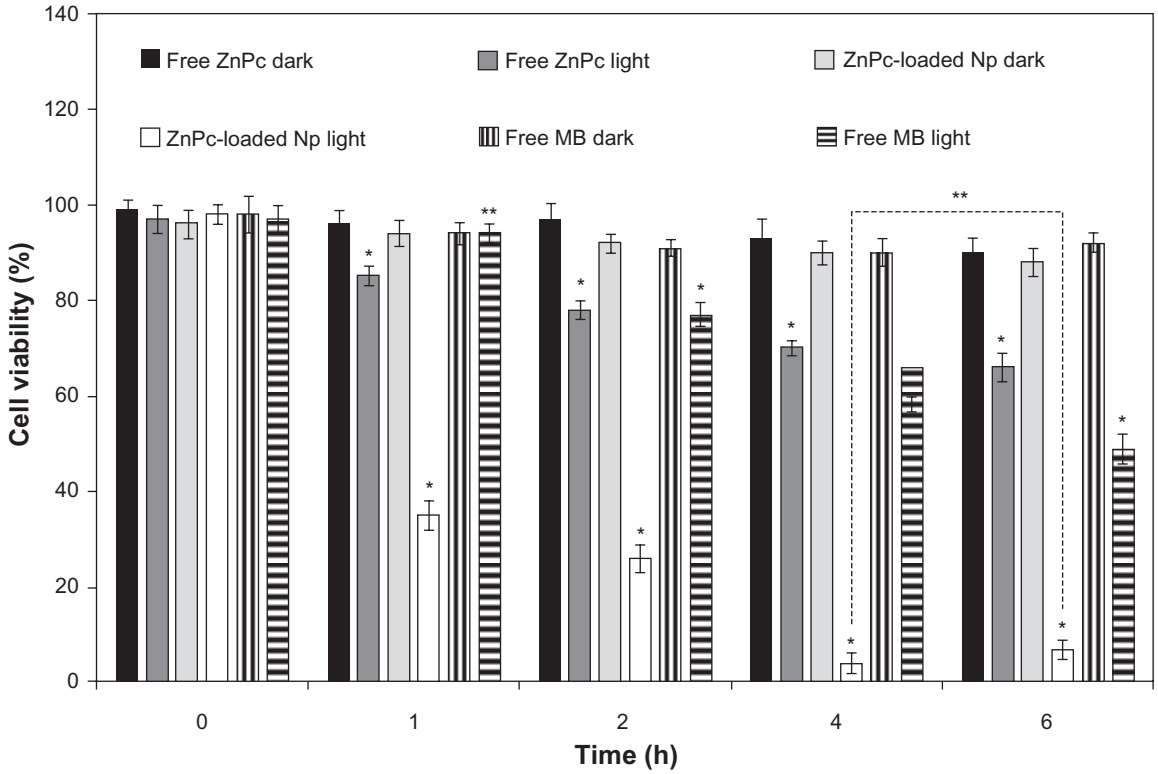

Figure 3 Influence of the incubation time (h) in the phototoxicity of free ZnPc or ZnPc-loaded nanoparticles. The cells were incubated with 5 μg (250 μL) of free ZnPc and ZnPc-loaded nanoparticles at different times, washed, and irradiated at a light dose of 100 J/cm^2. Dark toxicity was studied for all samples. The MTT assay was performed 24 h after light exposure. Each data point represents the mean (±SD) of n = 10 determinations.
Notes: *Significant difference ($P < 0.05$), **No significant difference ($P > 0.05$).
Abbreviations: ZnPc, zinc phthalocyanine; MTT, 3-(4,5-dimethyl-thiazol-2-yl)-2,5-biphenyl tetrazolium bromide; MB, methylene blue; SD, standard deviation.

in 5 and 10 μg/mL. ZnPc-loaded NPs exhibited phototoxicity significantly higher than free photosensitizers ($P < 0.05$) (Figure 4).

The influence of the light dose (J/cm^2) on the photobiological activity was evaluated using 5 μg of ZnPc (volume of 250 μL) and incubation time of 4 h. No toxicity was observed in the dark (without irradiation). Photobiological activity of the ZnPc-loaded NPs was observed at 10 J/cm^2. The light dose increase was responsible for the improvement of the biological effect. The free ZnPc exhibited photobiological activity in the light dose of 50–100 J/cm^2. Phototoxicity of the MB was observed at 20–100 J/cm^2. Besides, ZnPc-loaded NPs exhibited a phototoxic effect significantly higher than free photosensitizers ($P < 0.05$) (Figure 5).

No morphological change was observed in cells treated with saline (control group) (Figure 6A, B) and empty NPs (no photosensitizer) (Figure 6C, D) after illumination with visible light (red light, 660 nm, for 90 sec, with light dose of 100 J/cm^2). The cells incubated with NPs containing ZnPc and irradiated with visible light showed morphological changes. Morphological alterations of the cell induced by photobiological action of ZnPc included the following changes: cytoplasmic condensation with significant reduction of cell volume, rarified cytoplasmic matrix, extensive cell lysis, and loss of plasma membrane extensions (Figure 6E, F).

As shown in Figure 7, the chemical measurements showed a significant decrease in the absorbance at 400 nm for ZnPc-loaded NPs with ABMDMA after irradiation, suggesting a high efficiency in the generation of $^1O_2$ (Figure 7). For the free ZnPc, the photobleaching caused by $^1O_2$ was lower than that of ZnPc-loaded NPs. There was no decrease in the absorbance for a sample containing ABMDMA and empty NPs (Figure 7).

Discussion

NPs have been used as a possible method to target and control drug delivery, and prevent the side effects associated with undesirable biodistribution of the free form of drugs.[11,15] Moreover, there are many options for modifying the biodistribution of NPs by appropriate selection of the polymer, surface modification (hydrophilic coating), and particle size.[11] Among the morphofunctional features of solid tumors are the

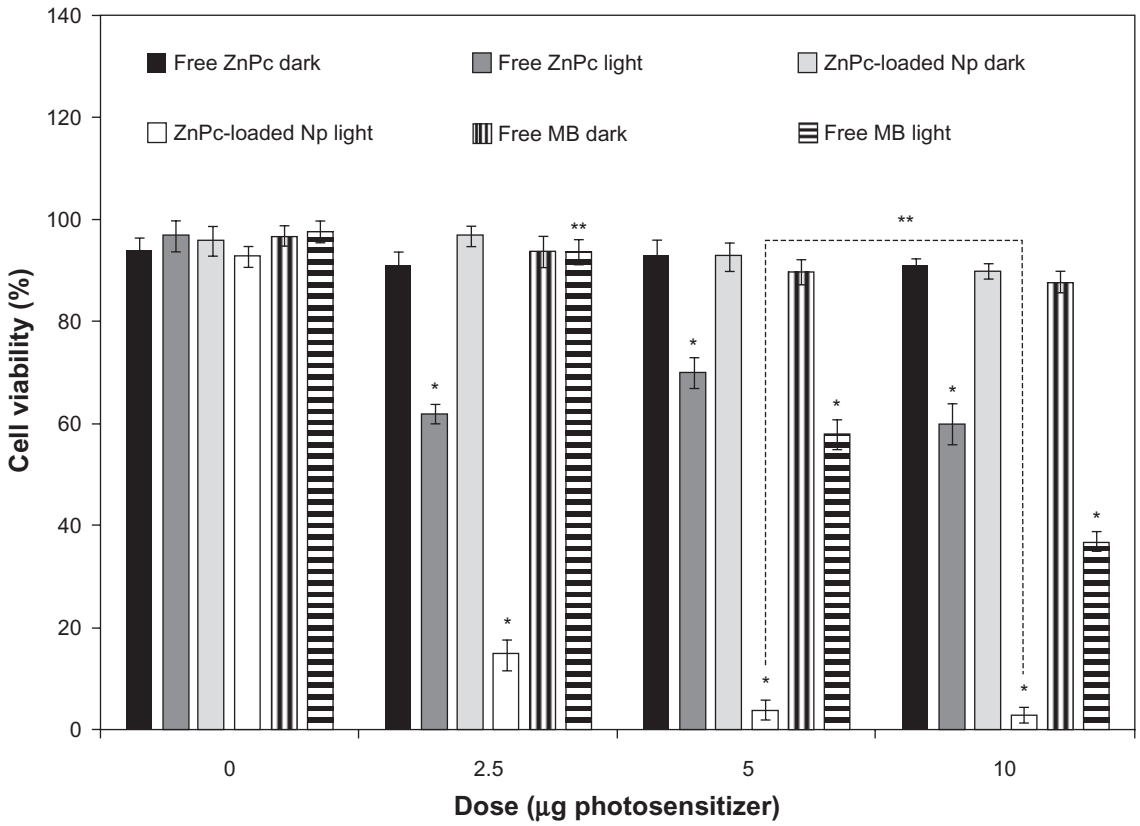

Figure 4 Influence of the photosensitizer concentration in the photobiological activity of free ZnPc, free MB, or ZnPc-loaded nanoparticles. The cells were incubated with 250 µL of free photosensitizer (ZnPc or MB) and ZnPc-loaded nanoparticles for 4 h, washed, and irradiated at a light dose of 100 J/cm^2. Dark toxicity was studied for all samples. The MTT assay was performed 24 h after light exposure. Each data point represents the mean (±SD) of n = 10 determinations.
Notes: *Significant difference ($P < 0.05$), **No significant difference ($P > 0.05$).
Abbreviations: ZnPc, zinc phthalocyanine; MB, methylene blue; MTT, 3-(4,5-dimethyl-thiazol-2-yl)-2,5-biphenyl tetrazolium bromide; SD, standard deviation.

abnormal function of the lymphatic vasculature, which causes fluid retention, and the increased permeability of blood vessel walls. Both these characteristics lead to a higher retention of NPs in the tumor area in comparison with normal tissues, resulting in a passive selectivity of the system.[42] Thus, nanometric size, which is directly related to the technique of NPs obtention, is crucial for the desired tissue penetration.[40]

The size of the NPs obtained depends on many factors such as the stirring speed, solution viscosity, organic/aqueous phase ratio, and surfactant concentration in the external aqueous phase. In this study, the use of solvent emulsification-evaporation method (SEEM) associated with sonication produced the photosensitizer-loaded NPs of appropriate size. NPs containing photosensitizer were produced with success using PCL by SEEM. The encapsulation method produced particles in nanometric scale (<200 nm) with narrow size distribution (IP < 0.1), spherical shape, and excellent EE (>60%). The low release depends on the nature of both the polymer and the encapsulated molecule.[38] ZnPc presented a low and sustained release. The release data were fitted using the mathematical models of zero order, first order, Higuchi, Hixon–Crowell, square root of mass, three seconds root of mass, and Baker–Lonsdale. Zero-order kinetics can be used to describe the drug release from several types of delivery systems such as matrix tablets for drugs with low solubility[44] and osmotic systems where drug release would be directly proportional to time. The first-order model describes the release profile from the delivery systems containing drugs dispersed in porous matrices where drugs would be released at rates proportional to the amount of drug remaining in the interior of the delivery system.[36] Hixon and Crowell recognized that the particle regular area is proportional to the cubic root of its volume.[45] This relationship between area and volume plus the release and remaining amount of the drug can influence the release kinetics. The shape factor for cubic or spherical particles should be kept constant if the particles are dissolved in an equal manner on all sides. When this model is used, it is assumed that the release rate is limited by the drug particle dissolution rate and not by the diffusion that might occur through the polymeric matrix.[45]

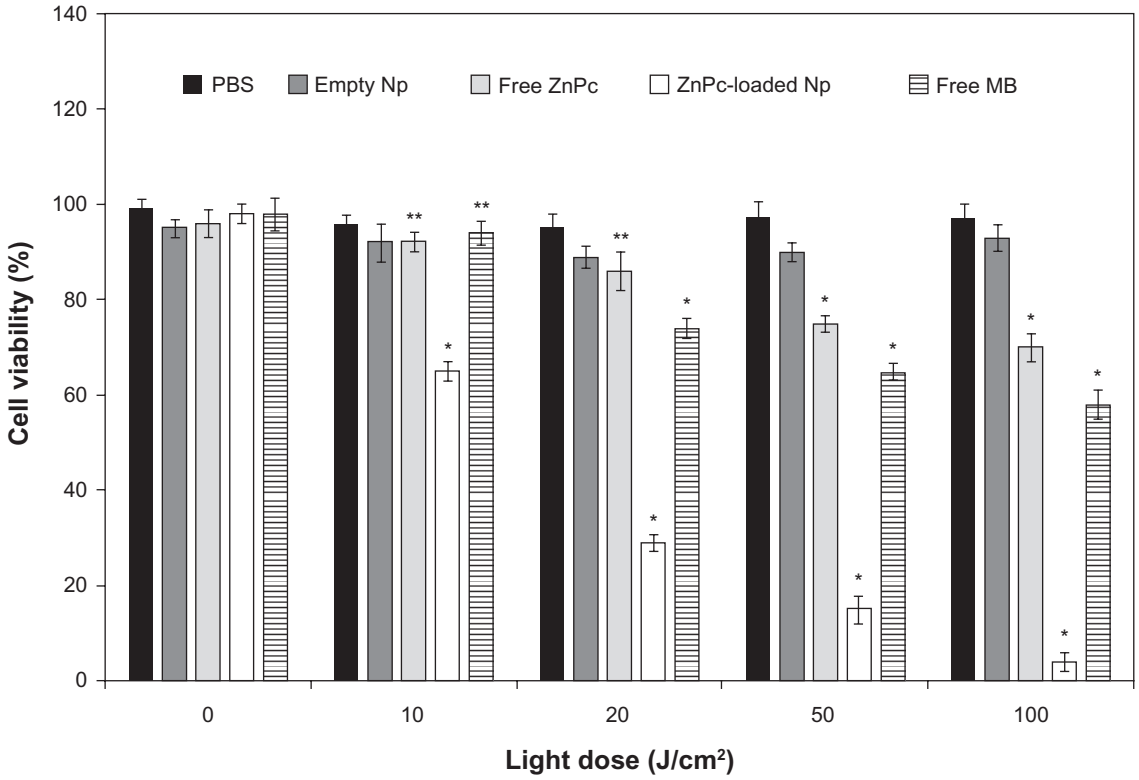

Figure 5 Influence of light dose on phototoxicity of free ZnPc and ZnPc-loaded nanoparticles. The cells were incubated for 4 h, at an equivalent drug dose of 5-pg ZnPc (250 μL), washed, and irradiated with red light (660 nm). MTT assay was performed 24 h after light exposure. Each data point represents the mean (±SD) of n = 10 determinations.

Notes: *Significant difference ($P < 0.05$), **No significant difference ($P > 0.05$).

Abbreviations: ZnPc, zinc phthalocyanine; MTT, 3-(4,5-dimethyl-thiazol-2-yl)-2,5-biphenyl tetrazolium bromide; SD, standard deviation.

The Baker–Lonsdale model was developed from the Higuchi model and describes drug controlled release from a spherical matrix.[46] This mathematical model has been used for linearization of release data from several formulations of microparticles and NPs. The mathematical models of squared root and three seconds root of mass were also tested in the release kinetic study.[36,37] The Higuchi model has been based on the Fick's law where the release occurs by the diffusion of drugs within the delivery system.[36,47] In this case, the released amount of the drug is proportional to the square root of time. The Higuchi model gave the highest value of R^2 and r, indicating that this mathematical model was the most suitable for describing the release of the photosensitizer from PCL NPs (Table 3). These results suggest that the release of ZnPc from PCL NPs is controlled by diffusion. From these results, the mechanism of the photosensitizer release from PCL NPs can be considered as follows: 1) Water penetrates into polymeric matrix of the NPs through pores, slowly dissolving the photosensitizer. 2) ZnPc is released by diffusion into acceptor solution. 3) The photosensitizer is hydrophobic and accumulates into SDS micelles.

The in vitro phototoxicity studies showed that the ZnPc-loaded NPs were more phototoxic than the free ZnPc (Figures 3–5). The photobiological activity is highly dependent on the photosensitizer's cellular uptake mechanism and its subcellular localization. In aqueous medium, a free lipophilic photosensitizer is generally absorbed by diffusion across the plasmatic membrane (lipophilic) leading to a low intracellular concentration. Moreover, lipophilic photosensitizers such as ZnPc tend to aggregate in aqueous medium with reduction of its photodynamic activity.[48] Due to its instability in water, the photobiological activity of the free ZnPc was not concentration dependent (Figure 4). The MB was less phototoxic than the ZnPc-loaded NPs ($P < 0.05$) (Figures 3–5). MB is hydrophilic and has difficulty in crossing the lipophilic membrane of the cells, leading to a low intracellular concentration. However, NPs are able to enter the cells by endocytosis, releasing the photosensitizer in the cell cytoplasm. The intracellular localization of the photosensitizer, an important factor in PDT, can induce different damage in the cells. Due to its hydrophobic characteristics, intracellular ZnPc is able to accumulate in the cytoplasmic

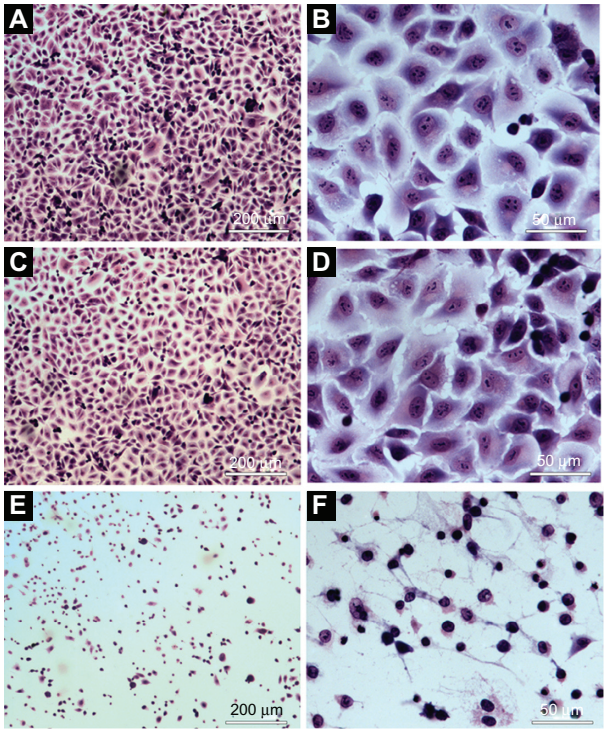

Figure 6 Morphological evaluation of the A549 cells using light microscope: **A**) and **B**) cells incubated with PBS (control). **C**) and **D**) cells incubated with empty nanoparticles suspension. **E**) and **F**) cells incubated with ZnPc-loaded nanoparticles. (A), (C), and (E) were observed at magnification of ×50 (scale 200 µm). (B), (I), and (F) were observed at magnification of ×400 (scale 50 µm).
Abbreviations: PBS, phosphate-buffered saline; ZnPc, zinc phthalocyanine.

membrane, lysosomal compartment, and mitochondria. Intracellular generation of $^1O_2$ and additional free radicals can act as potent cytotoxic agents.

The $^1O_2$ is the main toxic species generated by phthalocyanines during PDT.[49] The photobleaching studies (Figure 7) are in agreement with the photobiological activity

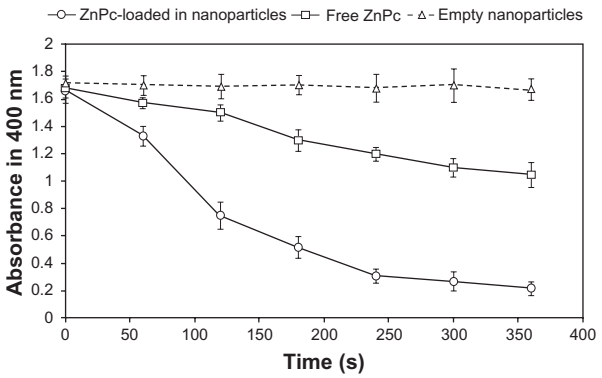

Figure 7 Photobleaching of ABMDMA by singlet oxygen generated by encapsulated ZnPc and free ZnPc. Empty nanoparticles were used as control. The change in ABMDMA absorption at 400 nm was measured as a function of the irradiation time. Each data point represents the mean (±SD) of n = 3 determinations.
Abbreviations: ABMDMA, 9,10-anthracenediyl-bis(methylene)dimalonic acid; ZnPc, zinc phthalocyanine; SD, standard deviation.

results (Figures 3–5). ZnPc-loaded NPs generated $^1O_2$ more efficiently than free ZnPc (Figure 7). The free ZnPc suffers aggregation in water leading to a low $^1O_2$ generation. However, encapsulation in NPs protected the ZnPc from the aggregation in aqueous medium. Due to slow release (Figure 2), many ZnPc molecules can remain adsorbed on the surface of the NPs. The adsorbed photosensitizer can be activated by red light leading to a strong $^1O_2$ generation. The photobleaching data are consistent with those obtained by Zhao et al.[50] The $^1O_2$ generation was improved after encapsulation of the lipophilic photosensitizer (silicon phthalocyanine (SiPc)) in silica NPs. SiPc is a lipophilic photosensitizer. It aggregates in aqueous solution, which reduces its therapeutic efficacy and limits its clinical use.[50] Zhao et al have encapsulated SiPc using silica NPs, which not only improves the aqueous stability but also increases its $^1O_2$ generation and photobiological activity compared with free SiPc.[50] SiPc-loaded silica NPs generated photo-induced $^1O_2$ more efficiently than free SiPc.[50]

The results obtained from in vitro phototoxicity studies demonstrated that the phototoxicity of ZnPc against the A549 cells occurred after 24 h of light exposure because the cellular damage resulting from the photochemical reaction is not immediately lethal. This phenomenon could be due to an apoptotic response, which is a slow process.[5] Cell death by necrosis[3] may occur on a smaller scale. Necrosis is a drastic process of death that results in cell lysis.

Conclusion

Nanotechnology is bringing new perspectives to a number of fields of human knowledge. Its applications in cancer treatment by PDT are being investigated largely with excellent results. The nanoencapsulation was suitable for the preparation of PCL NPs because the release system has nanometric size, narrow distribution, regular shape, and sustained release. Achieving optimal effect of PDT on tumor cells requires that the photosensitizer becomes closely associated to the subcellular organelles. Encapsulation of ZnPc in the PCL NPs improved its stability in aqueous medium and the in vitro phototoxicity. The photobiological activity was influenced by photodynamic parameters such as incubation time, light dose, and drug concentration. Based on all the photobiological measurements, it can be concluded that the ZnPc-loaded PCL NPs are promising delivery systems for use in PDT.

Acknowledgments

We thank the financial support of Conselho Nacional d Desenvolvimento Científico e Tecnológico (CNPq) and

Fundação Carlos Chagas Filho de Amparo à Pesquisa do Estado do Rio de Janeiro (FAPERJ).

Disclosure

The authors report no conflict of interest in this work.

References

1. Allison RR, Downie GH, Cuenca R, Hu XH, Childs CJH, Sibata CH. Photosensitizers in clinical PDT. *Photodiagnosis Photodyn Ther*. 2004;1:27–42.
2. Bechet D, Couleaud P, Frochot C, Viriot ML, Guillemin F, Barberi-Heyob M. Nanoparticles as vehicles for delivery of photodynamic therapy agents. *Trends Biotechnol*. 2008;26(11):612–621.
3. Castano AP, Demidova TN, Hamblin MR. Mechanisms in photodynamic therapy: Part three – Photosensitizer pharmacokinetics, biodistribution, tumor localization, and modes of tumor destruction. *Photodiagnosis Photodyn Ther*. 2005;2(2):91–106.
4. Chatterjee DK, Fong LS, Zhang Y. Nanoparticles in photodynamic therapy: an emerging paradigm. *Adv Drug Deliv Rev*. 2008;60(15):1627–1637.
5. Zhou C, Shunji C, Jinsheng D, Junlin L, Jori G, Milanesi C. Apoptosis of mouse MS-2 fibrosarcoma cells induced by photodynamic therapy with Zn (II)-phthalocyanine. *J Photochem Photobiol B*. 1996;33(3):219–223.
6. Bonnett R. Photosensitizers of the porphyrin and phthalocyanine series for photodynamic therapy. *Chem Soc Rev*. 1995;26(37):19–33.
7. Savolainen J, van der Linden D, Dijkhuizen N, Herek JL. Characterizing the functional dynamics of zinc phthalocyanine from femtoseconds to nanoseconds. *J Photochem Photobiol A Chem*. 2008;196(1):99–105.
8. Zanfolim AA, Volpati D, Olivati CA, Job AE, Constantino CJL. Structural and electric-optical properties of zinc phthalocyanine evaporate in films: temperature and thickness effects. *J Phys Chem*. 2010;114(28):12290–12299.
9. Ricci-Júnior E, Marchetti JM. Preparation, characterization, photocytotoxicity assay of PLGA nanoparticles containing zinc (II) phthalocyanine for photodynamic therapy use. *J Microencapsul*. 2006;23(5):523–538.
10. Wainwright M, Phoenix DA, Rice L, Burrow SM, Waring J. Increased cytotoxicity and phototoxicity in the methylene blue series via chromophore methylation. *J Photochen Photobiol B*. 1997;40(3):233–239.
11. Hans ML, Lowman AM. Biodegradable nanoparticles for drug delivery and targeting. *Curr Opin Solid State Mater Sci*. 2002;6(4):319–327.
12. Camerin M, Magaraggia M, Soncin M, et al. The in vivo efficacy of phthalocyanine–nanoparticle conjugates for the photodynamic therapy of amelanotic melanoma. *Eur J Cancer*. 2010;46(10):1910–1918.
13. Murthy SK. Nanoparticles in modern medicine: state of the art and future challenges. *Int J Nanomedicine*. 2007;2(2):129–141.
14. De Jong WH, Borm PJ. Drug delivery and nanoparticles: applications and hazards. *Int J Nanomedicine*. 2008;3(2):133–149.
15. Soppimath KS, Aminabhavi TM, Kulkarni AR, Rudzinski WE. Biodegradable polymeric nanoparticles as drug delivery devices. *J Control Release*. 2001;70(1–2):1–20.
16. Ungun B, Prud'homme RK, Budijon SJ, et al. Nanofabricated upconversion nanoparticles for photodynamic therapy. *Opt Express*. 2009;17(1):80–86.
17. Allison RR, Mota HC, Bagnato VS, Sibata CH. Bio-nanotechnology and photodynamic therapy–state of the art review. *Photodiagnosis Photodyn Ther*. 2008;5(1):19–28.
18. Konan YN, Berton M, Gurny R, Allemann E. Enhanced photodynamic activity of meso-tetra(4-hydroxyphenyl)porphyrin by incorporation into sub-200 nm nanoparticles. *Eur J Pharm Sci*. 2003;18(3–4):241–249.
19. Konan YN, Chevallier J, Gurny R, Allemann E. Encapsulation of p-THPP into nanoparticles: cellular uptake, subcellular localization and effect of serum on photodynamic activity. *Photochem Photobiol*. 2003;77(6):638–644.
20. Gomes AJ, Lunardi LO, Marchetti JM, Lunardi CN, Tedesco AC. Photobiological and ultrastructural studies of nanoparticles of poly(lactic-co-glycolic acid)-containing bacteriochlorophyll-*a* as a photosensitizer useful for PDT treatment. *Drug Deliv*. 2005;12(3):159–164.
21. Konan-Kouakou YN, Boch R, Gurny R, Allemann E. In vitro and in vivo activities of verteporfin-loaded nanoparticles. *J Control Release*. 2005;103(1):83–91.
22. Tang W, Xu H, Kopelman R, Philbert MA. Photodynamic characterization and in vitro application of methylene blue-containing nanoparticle platforms. *Photochem Photobiol*. 2005;81(2):242–249.
23. Zeisser-Labouebe M, Lange N, Gurny R, Delie F. Hypericin-loaded nanoparticles for the photodynamic treatment of ovarian cancer. *Int J Pharm*. 2006;326(1–2):174–181.
24. Allemann E, Rousseau J, Brasseur N, Kudrevich SV, Lewis K, van Lier JE. Photodynamic therapy of tumours with hexadecafluoro zinc phthalocyanine formulated in PEG-coated poly(lactic acid) nanoparticles. *Int J Cancer*. 1996;66(6):821–824.
25. Nair LS, Laurencin CT. Biodegradable polymers as biomaterials. *Prog Polym Sci*. 2007;32(8–9):762–798.
26. Sinha VR, Bansal K, Kaushik R, Kumria R, Trehan A. Poly-ε-caprolactone microspheres and nanosperes: an overview. *Int J Pharm*. 2004;278(1):1–23.
27. Kumari A, Yadav SK, Yadav SC. Biodegradable polymeric nanoparticles based drug delivery systems. *Colloids Surf B Biointerfaces*. 2010;75(1):1–18.
28. verger ML, Fluckiger L, Kim YI, Hoffman M, Maincent P. Preparation and characterization of nanoparticles containing an antihypertensive agent. *Eur J Pharm Biopharm*. 1998;46(2):137–143.
29. Ferranti V, Marchais H, Chabenat C, Orecchioni AM, Lafont O. Primidone-loaded poly-ε-caprolactone nanocapsules: incorporation efficiency and in vitro release profiles. *Int J Pharm*. 1999;193(1):107–111.
30. Kim SY, Lee YM. Taxol-loaded block copolymer nanospheres composed of methoxy poly(ethylene glycol) and poly(epsilon-caprolactone) as novel anticancer drug carriers. *Biomaterials*. 2001;22(13):1697–1704.
31. Zili Z, Sfar S, Fessi H. Preparation and characterization of poly-ε-caprolactone nanoparticles containing griseofulvin. *Int J Pharm*. 2005;294(1–2):261–267.
32. Shenoy DB, Amiji MM. Poly(ethylene-oxide)-modified poly(ε-caprolactone) nanoparticles for targeted delivery of tamoxifen in breast cancer. *Int J Pharm*. 2005;293(1–2):261–270.
33. Blouza IL, Charcosset C, Sfar S, Fessi H. Preparation and characterization of spironolactone-loaded nanocapsules for pediatric use. *Int J Pharm*. 2006;325(1–2):124–131.
34. Prabu P, Chaudhari AA, Dharmaraj N, Khil MS, Park SY, Kim HY. Preparation, characterization, in-vitro drug release and cellular uptake of poly(caprolactone) grafted dextran copolymeric nanoparticles loaded with anticancer drug. *J Biomed Mater Res*. 2009;90(4):1128–1136.
35. Zheng D, Li X, Xu H, Lu X, Hu Y, Fan W. Study on docetaxel-loaded nanoparticles with high antitumor efficacy against malignant melanoma. *Acta Biochim Biophys Sin*. 2009;41(7):578–587.
36. Costa P, Sousa Lobo JM. Modeling and comparison of dissolution profiles. *Eur J Pharm Sci*. 2001;13(2):123–133.
37. Barzegar-Jalali M, Adibkia K, Valizadeh H, et al. Kinetic analysis of drug release from nanoparticles. *J Pharm Pharm Sci*. 2008;11(1):167–177.
38. Lieber M, Smith B, Szakal A, Nelson-Rees W, Todaro G. A continuous tumor-cell line from a human lung carcinoma with properties of type II alveolar epithelial cells. *Int J Cancer*. 1976;17(1):62–70.

39. Mosmann T. Rapid colorimetric assay for cellular growth and survival: application to proliferation and cytotoxicity assays. *J Immunol Methods*. 1983;65(1–2):55–63.
40. Veiga VF, Nimrichter L, Teixeira CA, et al. Exposure of human leukemic cells to direct electric current: generation of toxic compounds inducing cell death by different mechanisms. *Cell Biochem Biophys*. 2005;42(1):61–74.
41. Lindig BA, Rodgers MAJ, Schaap AP. Determination of the lifetime of singlet oxygen in D_2 using 9,10-anthracenedipropionic acid, a water-soluble probe. *J Am Chem Soc*. 1980;102(17):5590–5593.
42. Alexis F, Rhee JW, Richie JP, Radovic-Moreno AF, Langer R, Farokhzad OC. New frontiers in nanotechnology for cancer treatment. *Urol Oncol*. 2008;26(1):74–85.
43. Kong G, Braun RD, Dewhirst MW. Hyperthermia enables tumor-specific nanoparticle delivery: effect of particle size. *Cancer Res*. 2000; 60(16):4440–4445.
44. Tanaka N, Imai K, Okimoto K, et al. Development of novel sustained-release system, disintegration-controlled matrix tablet (DCMT) with solid dispersion granules of nilvadipine. *J Control Release*. 2005; 108(2–3):386–395.
45. Hixson AW, Crowell JH. A simple model based on first order kinetics to explain release of highly water. *Ind Eng Chem Res*. 1931;23: 923–931.
46. Baker RW, Lonsdale HS. *Controlled Release of Biologically Active Agents*. Tanquary AC, Lacey RE, editors. New York, NY: Plenum Press; 1974.
47. Higuchi T. Mechanism of sustained-action medication: theoretical analysis of rate of release of solid drugs dispersed in solid matrices. *J Pharm Sci*. 1963;52:1145–1149.
48. Isele U, Schieweck K, Kessler R, van Hoogevest P, Capraro HG. Pharmacokinetics and body distribution of liposomal zinc phthalocyanine in tumor-bearing mice: influence of aggregation state, particle size, and composition. *J Pharm Sci*. 1995;84(2):166–173.
49. Allen CM, Sharman WM, van Lier JE. Current status of phthalocyanines in the photodynamic therapy of cancer. *J Porphyr Phthalocyanines*. 2001;5:161–169.
50. Zhao B, Yin JJ, Bilski PJ, Chignell CF, Roberts JE, He Y-Y. Enhanced photodynamic efficacy towards melanoma cells by encapsulation of Pc4 in silica nanoparticles. *Toxicol Appl Pharmacol*. 2009;241(2): 163–172.